

# Any2Any: Efficient Cross-Embodiment Transfer for Humanoid Whole-Body Tracking

Ming Yang<sup>1</sup>, Tao Yu<sup>1,†,\*</sup>, Feng Li<sup>1</sup>, Hua Chen<sup>1,\*</sup>

<sup>1</sup>LimX Dynamics

<sup>†</sup>Project Lead \*Corresponding Authors

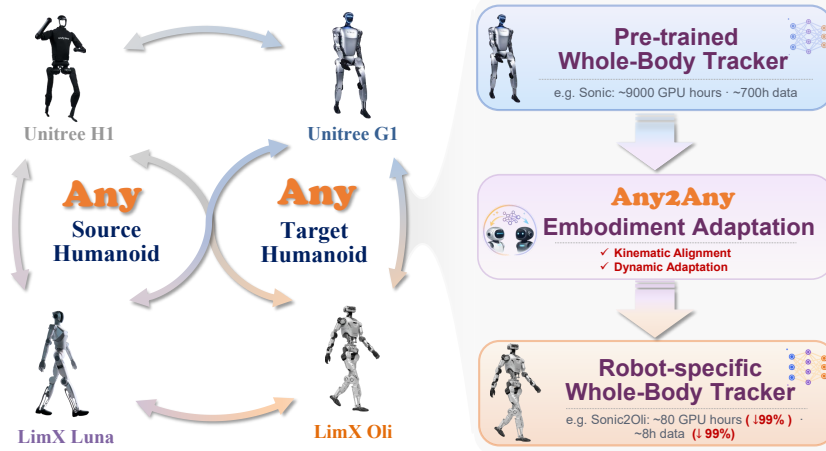


Figure 1: Illustration of ANY2ANY. A pretrained whole-body tracker (WBT) learned on specific humanoid can be efficiently transferred to another humanoid platform through the proposed ANY2ANY. For example, GEAR-SONIC [1], a large-scale pretrained WBT, can be adapted to a target robot LimX Oli using only a small fraction of the original training compute and data.

## Abstract:

Whole-body tracking (WBT) models have become a key foundation for humanoid robots, enabling them to imitate diverse motions with high fidelity. Training such models from scratch requires large-scale data and computation, making rapid deployment on new humanoid platforms costly. This raises a natural question: *Can pretrained WBT models transfer across embodiments with minimal adaptation?* To answer this question, we propose ANY2ANY, a paradigm that efficiently transfers an existing WBT specialist to a new humanoid embodiment with only a small amount of data and compute. Any2Any first performs *kinematic alignment* between source and target humanoids, aligning their input and output spaces so that the pretrained source policy can be meaningfully reused on the target embodiment. ANY2ANY then performs *dynamics adaptation* by applying lightweight parameter-efficient fine-tuning (PEFT) components to selected dynamics-sensitive modules, preserving useful behavioral priors while enabling targeted adaptation to the target robot. Extensive experiments on multiple humanoid platforms and pretrained backbones show that ANY2ANY substantially accelerates convergence and reduces training cost compared with training from scratch, while achieving competitive or superior tracking performance. Notably, using only 1% of the compute and data required for full training, Any2Any successfully transfers Sonic models pre-trained on Unitree G1 to LimX Oli and LimX Luna. These results suggest that pretrained WBT specialists can be efficiently reused across embodiments, providing a scalable path toward deploying humanoid whole-body control on new robots.

# 1 Introduction

Behavior foundation models (BFMs) are emerging as a promising paradigm for humanoid control [2, 3]. By pretraining on large-scale behavior data, BFMs aim to acquire reusable motor skills and broad behavioral priors that can be rapidly adapted to downstream tasks [4, 5]. For humanoid robots, whole-body tracking (WBT) is a natural BFM-style control interface: the policy learns to reproduce diverse full-body reference motions while coordinating legs, torso, arms, and head to maintain balance [6, 7]. A large-scale WBT policy can therefore serve as a reusable whole-body motor prior for teleoperation, motion imitation, and downstream loco-manipulation [8, 9, 10, 1].

Recent humanoid WBT systems have increasingly followed this scaling trend. TWIST and GMT demonstrate that end-to-end WBT policies can cover diverse whole-body motions through reinforcement learning, behavior cloning, teacher-student training, adaptive sampling, and mixture-of-experts designs [9, 10]. SONIC further frames motion tracking as a scalable foundation task, scaling the policy from 1.2M to 42M parameters, using over 100M motion frames, and reporting 9k GPU hours of training [1]. These results mark important progress toward general humanoid motor priors, but they also expose a practical barrier: reproducing such natural and robust whole-body behaviors requires large-scale motion data, massively parallel simulation infrastructure, and substantial compute budgets.

Beyond training cost, embodiment dependence remains a fundamental limitation of current large-scale WBT policies [11, 12]. Such policies are tightly coupled to the source robot’s morphology, actuator configuration, and sensor interface, so even between similar humanoids the resulting structural and dynamical differences make direct deployment unreliable and direct full-policy fine-tuning prone to overwriting the source behavioral prior. Existing cross-embodiment methods mainly address this issue by training universal controllers over many embodiments with morphology randomization or multi-embodiment data [13, 14, 15], or by scaling robot foundation models with embodiment-aware representations, unified action spaces, post-training, or expert routing [16, 17, 18]. However, these approaches typically require large scale multi-embodiment datasets, broad morphology randomization, or expensive large-scale pretraining from scratch. In contrast, we study a complementary post-training problem: given a mature WBT policy trained on one humanoid, can we efficiently adapt it to another humanoid with limited data and compute?

A long-standing principle in humanoid control is to decouple kinematics from dynamics: classical pipelines typically plan a kinematic reference and track it with a hierarchical whole-body controller [19, 20], while learning-based whole-body tracking (WBT) policies often encode retargeted reference motions [21] separately from the dynamics-aware control stream [1]. This decoupling also reveals the structure of cross-embodiment transfer. A source policy trained on one humanoid differs from a target humanoid along two distinct axes. *Kinematically*, the two robots may have different joint counts, link geometries, and observation/action layouts, making the pretrained policy structurally incompatible with the target embodiment. *Dynamically*, they differ in mass distributions, inertias, actuator responses, and contact behaviors, so even after interface alignment, the source policy may still produce suboptimal or incorrect actions on the target. Adapting to this dynamics gap requires parameter updates, but directly fine-tuning the full policy risks overwriting the source behavioral prior that makes the pretrained policy valuable. Encouragingly, this kinematics-dynamics separation is also reflected in modern WBT network designs, which commonly adopt a two-stream structure consisting of a Reference Motion Encoder and an Action Decoder [9, 10, 1, 22, 23, 24]. The encoder primarily extracts motion-related, largely kinematic features that are more transferable across embodiments, whereas the decoder is more tightly coupled to embodiment-specific dynamics. We therefore hypothesize that embodiment changes affect different components of the WBT prior unevenly: global motor skills such as balance and inter-limb coordination may remain broadly reusable, while embodiment-sensitive modules require adaptation. This motivates a localized adaptation strategy, where lightweight PEFT components such as LoRA and adapters [25, 26, 27, 28] are inserted only into modules with the largest source-target discrepancy, while the remaining parameters are frozen to preserve the source prior. This leads to three key questions: *Can localized fine-tuning adapt to the target embodiment without destroying the source prior? How should the*

*kinematic mismatch be resolved? Which modules should be adapted to maximize cross-embodiment transfer?*

To answer these questions, we propose ANY2ANY, a parameter-efficient post-training framework that decomposes cross-embodiment WBT transfer into two aspects: *kinematic alignment*, which remaps the source and target input-output spaces, and *dynamic adaptation*, which uses lightweight PEFT components to update only the dynamics-sensitive modules. We study where adaptation should be localized and validate ANY2ANY across multiple source-target transfer pairs. Our contributions are threefold:

1. We demonstrate that humanoid WBT policies pretrained on a single source robot can be effectively transferred to other humanoid embodiments through principled handling of the kinematic and dynamic mismatches. To the best of our knowledge, this constitutes the first systematic study of cross-embodiment transfer for humanoid WBT.
2. We propose ANY2ANY, a cross-embodiment post-training framework for humanoid WBT that decomposes transfer into *kinematic alignment*, which resolves the structural input-output mismatch between source and target robots, and *dynamic adaptation*, which selectively adapts only the dynamics-sensitive modules, while keeping the rest of the pretrained backbone frozen.
3. We validate ANY2ANY on five source-target transfer pairs spanning two pretrained WBT backbones and four target humanoid embodiments, achieving successful transfer with only  $\sim 1\%$  of the compute and data of full training, and deploy the resulting policies on real hardware across multiple downstream tasks.

## 2 Related Works

**Humanoid Whole-Body Tracking.** Humanoid control has progressed from task-specific motion imitation to large-scale whole-body tracking (WBT). DeepMimic [29] demonstrates that physics-based reinforcement learning can imitate reference motions and produce natural full-body behaviors, while PHC [30] improves scalable humanoid motion tracking from large-scale unstructured human motion data. Recent studies further extend WBT to real humanoids, including teleoperation [9], general motion tracking [10], long-horizon closed-loop control [31], and balance-intensive motions [32]. SONIC scales this paradigm with larger policies and motion datasets, showing the potential of WBT as a foundation-level motor interface [1]. However, these policies are still trained and tuned for a specific robot embodiment [32, 33, 34]. Their observation layout, action space, reward design, and dynamics randomization are tightly coupled to one morphology. In contrast, ANY2ANY studies how to transfer an existing WBT policy and efficiently adapt it to a different humanoid embodiment.

**Cross-Embodiment Robot Learning.** Cross-embodiment learning aims to share control knowledge across robots with different morphologies. Existing methods commonly train generalist controllers over multiple embodiments using morphology randomization [13], topology-aware architectures [35], unified observation-action spaces [15], or residual adaptation modules [14]. In robot foundation models, cross-embodiment generalization is often addressed through large-scale cross-embodiment pretraining [36, 37], embodiment-aware architectures [38], and unified action/state representations with expert routing [39, 18]. These methods are powerful, but they typically require multi-embodiment datasets, broad robot coverage, and expensive training from scratch. This is difficult for WBT, where high-quality specialist policies already require substantial data and compute. ANY2ANY addresses a complementary setting: given one pretrained WBT specialist, we transfer it to a target humanoid through kinematic Alignment and lightweight policy adaptation, without rebuilding a multi-robot generalist model.

**Parameter-Efficient Fine-tuning for Robotics.** A direct way to adapt a pretrained model is full fine-tuning, which updates all model parameters for the target domain [40]. Parameter-efficient

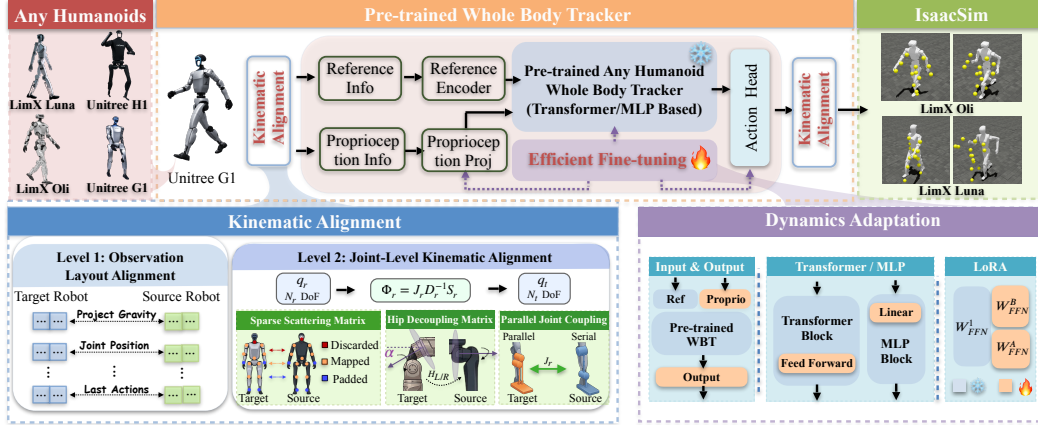


Figure 2: **Architecture of ANY2ANY.** The proposed framework adapts a pretrained whole-body tracker to arbitrary humanoid embodiments by combining **Kinematic Alignment**, which maps observations and actions across different robot morphologies, with **Dynamics Adaptation**, which efficiently fine-tunes lightweight modules to account for target-specific dynamics.

fine-tuning instead freezes most pretrained weights and updates only a small set of task-specific parameters. Adapter tuning inserts trainable bottleneck modules [41]; Prefix-Tuning optimizes continuous prefix tokens while keeping the backbone frozen [28]; LoRA represents weight updates with low-rank factors [26]. Recent works have begun to adapt PEFT techniques to robotic foundation models, enabling efficient specialization to downstream tasks and embodiments without retraining the entire policy [42, 43]. However, adapting a closed-loop humanoid WBT policy is fundamentally different from adapting a static prediction model: small parameter changes can propagate through contact dynamics, balance regulation, and action feedback, leading to non-trivial shifts in the resulting state distribution. It therefore remains unclear which PEFT mechanism and where PEFT components should be inserted, and to what extent the motion priors encoded in an existing WBT policy can be reused on a structurally different humanoid. In this work, ANY2ANY aims to fill this gap by introducing a systematic paradigm tailored for humanoid whole-body tracking, which transfers pretrained WBT policy to new humanoids with only a small amount of adaptation data and computational resources.

### 3 Method

#### 3.1 Problem Formulation

We formulate humanoid whole-body tracking (WBT) as a Markov Decision Process (MDP)  $\mathcal{M} = (\mathcal{X}, \mathcal{A}, \mathcal{P}, r, \gamma)$ , with state space  $\mathcal{X}$ , action space  $\mathcal{A}$ , transition kernel  $\mathcal{P}$ , reward  $r$ , and discount  $\gamma$ . For a given robot embodiment,  $\mathcal{X}$  and  $\mathcal{A}$  are determined by its morphological properties (number of actuated joints, kinematic structure, link masses, inertias, actuator gains) and by the specific tracking task.

Let  $\mathcal{E}_S$  denote a source robot equipped with a pretrained WBT policy  $\pi_{\theta_S} : \mathcal{X}_S \rightarrow \mathcal{A}_S$ , where  $\theta_S$  is its full parameter set. For a target robot  $\mathcal{E}_T$ ,  $\mathcal{X}_S \neq \mathcal{X}_T$  and  $\mathcal{A}_S \neq \mathcal{A}_T$  due to differences in joint configuration and degrees of freedom. Re-training the full parameter set  $\theta_S$  on  $\mathcal{E}_T$  is computationally expensive and risks catastrophic forgetting of the transferable motor priors encoded in  $\theta_S$ .

We instead freeze  $\theta_S$  and learn a small target-specific adaptation  $\Delta\theta_T$  with  $|\Delta\theta_T| \ll |\theta_S|$ . The resulting target policy is

$$\pi_{\theta_T}(a_t | s_t) = \pi_{\theta_S \oplus \Delta\theta_T}(a_t | s_t), \quad (1)$$

where  $\oplus$  denotes the parameter-efficient injection of  $\Delta\theta_{\mathcal{T}}$  into selected modules of the frozen backbone. The adaptation is trained under the standard expected-return objective

$$\max_{\Delta\theta_{\mathcal{T}}} \mathbb{E}_{\pi_{\theta_{\mathcal{T}}}} \left[ \sum_{t=0}^T \gamma^t r(s_t, a_t) \right]. \quad (2)$$

Different PEFT mechanisms such as LoRA, Adapter, and Prefix Tuning realize the operator  $\oplus$  at different locations within the network, yielding distinct trade-offs in parameter efficiency, training stability, and tracking quality. Identifying which positions and mechanisms yield the most effective cross-embodiment WBT adaptation under limited data and compute is the focus of this work.

### 3.2 Pretrained Whole Body Tracking Policy Structure

We adopt an actor-critic framework trained with Proximal Policy Optimization (PPO) for motion imitation. The actor  $\pi_{\theta}$  outputs target joint position offsets, while the critic  $V_{\phi}$  estimates state values using privileged observations (e.g., base velocity, contact forces, body mass distribution) that are available only during training. To demonstrate the generalizability of the proposed method, we instantiate the actor with three representative policy backbones that share a unified observation formulation but differ in how they encode and aggregate the inputs. The first two backbones are trained under the Oli whole-body tracking setting and are collectively referred to as **Oli-WBT**.

**Unified Observation Formulation.** At each control step  $t$ , the policy input is organized into two components: proprioceptive feedback and reference motion information.

- **Proprioception:** the robot-centric state, including base angular velocity, projected gravity, joint positions, joint velocities, and the previous action. These observations provide feedback about the current physical state and recent control history of the robot.
- **Reference:** the target motion state extracted from the reference trajectory, which provides task-level guidance for motion imitation.

**MLP Backbone.** The MLP policy flattens multi-modal observations over  $H + 1$  timesteps into a vector of dimension  $(H + 1)(d_p + d_r)$ , which is then processed by an  $L$ -layer MLP with GELU activations to predict actions. The critic uses the same architecture with privileged observations as input. This simple yet effective design is widely adopted in recent humanoid whole-body tracking works [8, 7].

**Transformer Backbone.** The Transformer policy models temporal dependencies by projecting each modality into a shared  $d$ -dimensional embedding space and processing the resulting sequence with  $N$  causal Transformer Decoder blocks. The action is decoded from the current-timestep representation, while the critic follows the same architecture with privileged observations.

**Sonic Backbone.** We further adopt Sonic [1] as a representative large-scale humanoid motion tracking architecture. In our experiments, we employ its Robot Motion Encoder, FSQ bottleneck, and dynamics decoder modules for training and evaluation. More architectural details can be found in [1].

### 3.3 Cross-Embodiment Adaptation

Since the source and target robots may differ in their degrees of freedom ( $n_j^S \neq n_j^T$ ), their observation and action spaces cannot be directly shared. Before applying any PEFT method, we introduce a kinematic alignment step to construct a unified joint-level representation across embodiments.

#### 3.3.1 Kinematic Alignment

To bridge the embodiment gap between the source and target robots before any parameter adaptation, we introduce a two-level kinematic alignment module that operates on the policy’s input and output streams (Fig. 2). The first level aligns the *global observation layout*, while the second level aligns the

*joint-level kinematic representation.* Together, they guarantee that the frozen source policy always receives observations with a consistent semantic layout and a compatible joint ordering, while the target robot still executes actions in its own control convention.

**Level 1: Observation Layout Alignment.** Different humanoid platforms typically organize their observation vectors in different orders, even when the underlying entries are semantically equivalent. At this level, we rearrange each component of the target robot’s observation, such as projected gravity, joint positions, and last actions, to match the input convention of the pretrained source policy. This ensures that semantically equivalent terms, including base states, reference motion features, proprioceptive states, and action history, are placed at consistent positions in the observation vector consumed by the frozen backbone.

**Level 2: Joint-Level Kinematic Alignment.** The second level aligns the internal ordering and geometry of joint-related variables. Consider a family of robots  $\mathcal{R} = \{r_1, r_2, \dots\}$  that share the same humanoid topology but differ in joint count, where each robot  $r$  has  $N_r$  degrees of freedom. We treat the joint layout of the pretrained source robot  $r_0$ , with  $N_{r_0} = T$ , as a unified kinematic semantic space, and for every  $r \in \mathcal{R}$  we construct a pair of mappings  $\Phi_r : \mathbb{R}^{N_r} \rightarrow \mathbb{R}^T$  and  $\Phi_r^+ : \mathbb{R}^T \rightarrow \mathbb{R}^{N_r}$  between the target and source joint spaces, satisfying  $\Phi_r^+ \Phi_r = I_{N_r}$ . The mapping  $\Phi_r$  is composed of three structured components that progressively account for joint-level discrepancies between the two embodiments.

**(i) Sparse Scattering Matrix.** Joint correspondence between the target and source robots is specified by an injection  $\pi_r : \{0, \dots, N_r - 1\} \hookrightarrow \{0, \dots, T - 1\}$ , which induces a sparse scattering matrix  $S_r \in \{0, 1\}^{T \times N_r}$  with  $(S_r)_{ij} = \mathbf{1}[\pi_r(j) = i]$ . Each column of  $S_r$  has exactly one nonzero entry, so  $S_r$  scatters target-space values into the source layout, padding zeros at positions without a target counterpart; redundant target joints are discarded by being excluded from the domain of  $\pi_r$ .

**(ii) Hip Decoupling Matrix.** The source embodiment contains an inclined hip-pitch axis, which induces a coupling between the corresponding hip coordinates. To compensate for this structural difference, we introduce a hip decoupling matrix  $D_r \in \mathbb{R}^{T \times T}$ . Specifically,  $D_r$  is initialized as a  $T \times T$  identity matrix, and its left and right hip submatrices are replaced by the following decoupling blocks:

$$H_{L/R} = \begin{pmatrix} \cos \alpha & 0 \\ \mp \sin \alpha & 1 \end{pmatrix}, \quad (3)$$

where the opposite signs account for the mirrored hip-axis orientations on the left and right legs. In this way,  $D_r$  acts only on the hip-related coordinates and leaves all other joints unchanged.

Combining the scattering matrix  $S_r$  and the hip decoupling matrix  $D_r$  gives the aligned forward and inverse mappings

$$\Phi_r = D_r^{-1} S_r, \quad \Phi_r^+ = S_r^\top D_r. \quad (4)$$

Here,  $S_r$  first scatters target-robot joint quantities into the source joint layout, and  $D_r^{-1}$  further converts the hip coordinates into the source-aligned convention. Conversely,  $D_r$  maps the policy output back from the source-aligned convention, and  $S_r^\top$  gathers the corresponding entries for the target robot.

Structured joint-related terms in the observation, including reference motion, joint position observations, and action history, are mapped to the source space via  $\tilde{\mathbf{q}}_r = \Phi_r \mathbf{q}_r$ . The same rule is applied to the action space: the policy output  $\tilde{\mathbf{a}}$  produced under the source-aligned joint convention is converted back to the target robot’s actuated joints through  $\mathbf{a}_r = \Phi_r^+ \tilde{\mathbf{a}}$  for execution.

**(iii) Parallel Joint Coupling.** Beyond serial-chain joint correspondence, some target robots contain closed-chain mechanisms, such as parallelogram-driven ankles or closed-loop waists, whose actuated joint values do not coincide with their kinematic counterparts in the source serial chain. For these joints, we incorporate a closed-chain Jacobian correction  $J_r \in \mathbb{R}^{T \times T}$  into the mapping, so that the effective joint-level alignment becomes

$$\Phi_r = J_r D_r^{-1} S_r, \quad \Phi_r^+ = S_r^\top D_r J_r^{-1}, \quad (5)$$

which preserves the invertibility relation  $\Phi_r^+ \Phi_r = I_{N_r}$ . This term explicitly handles parallel-to-serial discrepancies that purely permutation-based alignment cannot capture.

Through these two levels of alignment, the frozen source policy operates on a stable kinematic semantic space, while embodiment-specific details, such as joint ordering, hip-axis inclination, and closed-chain coupling, are absorbed by the alignment module itself. This consistently reduces the embodiment gap before parameter adaptation, and provides a more reliable basis on which subsequent PEFT methods can specialize the policy to the target humanoid.

### 3.3.2 Dynamic Adaptation

Once kinematic alignment is in place, the remaining gap between the source embodiment  $\mathcal{S}$  and the target embodiment  $\mathcal{T}$  is no longer representational but *dynamical*. Here,  $\mathcal{S}$  denotes the humanoid embodiment on which the whole-body tracker is originally pretrained, while  $\mathcal{T}$  denotes the new target humanoid embodiment to which the tracker is transferred. After kinematic alignment, we use  $q$  to denote the joint state expressed in the shared source-aligned joint convention. The rigid-body dynamics of a humanoid admits the standard manipulator-equation form

$$M(q) \ddot{q} + C(q, \dot{q}) \dot{q} + G(q) = \tau + \tau_{\text{ext}}, \quad (6)$$

which makes explicit that an embodiment’s physical identity is carried by three state-dependent terms: the mass matrix  $M(q)$ , the Coriolis/centrifugal coupling  $C(q, \dot{q})$ , and the gravity loading  $G(q)$ . Under the same motion target  $(q, \dot{q}, \ddot{q})$ , two humanoids with different dynamics  $(M_{\mathcal{S}}, C_{\mathcal{S}}, G_{\mathcal{S}})$  and  $(M_{\mathcal{T}}, C_{\mathcal{T}}, G_{\mathcal{T}})$  require different generalized forces to realize that motion, yielding the rigid-body residual

$$\Delta\tau(q, \dot{q}, \ddot{q}) = \Delta M(q) \ddot{q} + \Delta C(q, \dot{q}) \dot{q} + \Delta G(q), \quad (7)$$

where  $\Delta M = M_{\mathcal{T}} - M_{\mathcal{S}}$ ,  $\Delta C = C_{\mathcal{T}} - C_{\mathcal{S}}$ , and  $\Delta G = G_{\mathcal{T}} - G_{\mathcal{S}}$ . Beyond these rigid-body terms, the realized force-motion relation also depends on non-modeled effects such as actuator characteristics, joint friction, and contact behavior, which contribute additional residual components on top of  $\Delta\tau$ . Collecting all embodiment-specific physical quantities into a single descriptor  $\eta_e$ , the full cross-embodiment dynamics gap can be characterized by

$$\Delta\eta = \eta_{\mathcal{T}} - \eta_{\mathcal{S}}. \quad (8)$$

For humanoids of similar topology and scale,  $\Delta\eta$  is structurally low-dimensional: only a limited subset of physical quantities differ between the two robots, and the rigid-body part  $(\Delta M, \Delta C, \Delta G)$  is fully parameterized by per-link inertial differences whose number scales with the link count rather than with the size of the full backbone  $\theta_{\mathcal{S}}$ . After kinematic alignment removes the dominant structural mismatch,  $\Delta\eta$  becomes the primary remaining source of embodiment-dependent policy mismatch. Since this residual is compact relative to the full pretrained policy, we adapt the target robot through a low-rank, embodiment-specific correction instead of full-parameter fine-tuning. The pretrained policy has already captured the task structure (reference tracking, balance, inter-limb coupling) in a source-aligned representation; what remains is to learn a compact, embodiment-specific correction whose capacity matches  $\Delta\eta$  rather than  $\theta_{\mathcal{S}}$ . Such a correction can be naturally understood as a learned representation of the source-target dynamics residual, rather than as a generic perturbation of the source weights.

This motivates a strongly asymmetric adaptation: we freeze the pretrained parameters  $\theta$  and learn an embodiment-specific low-rank correction. Concretely, for each adapted linear projection  $W \in \mathbb{R}^{d_{\text{out}} \times d_{\text{in}}}$  in the policy, we apply a LoRA decomposition

$$W' = W + BA, \quad A \in \mathbb{R}^{k \times d_{\text{in}}}, B \in \mathbb{R}^{d_{\text{out}} \times k}, \quad (9)$$

with rank  $k \ll \min(d_{\text{in}}, d_{\text{out}})$ . Only  $\{A, B\}$  are trained per target embodiment, while  $W$  remains shared with the source. The rank  $k$  controls how much capacity is allocated to absorbing the cross-embodiment dynamics gap, providing a tunable trade-off between transfer fidelity and adaptation cost.

Together with the kinematic alignment, this design factorizes the cross-embodiment gap into a fixed structural component absorbed by the alignment, and a learned dynamical component absorbed by LoRA, keeping the source policy’s behavioral prior still while allowing each new embodiment to be specified by a small set of low-rank factors.

### 3.4 Training Procedure

All policies are trained with PPO in Isaac Lab. To isolate the effect of cross-embodiment adaptation, we keep the action space, observations, reward formulation, PPO hyperparameters, reference-motion sampling, and domain randomization protocol identical to those of the corresponding source pretraining setup, only the components introduced by our kinematic alignment and dynamic adaptation differ.

## 4 Experimental Results

In this section, our experimental evaluations are designed to thoroughly assess the proposed ANY2ANY framework in cross-embodiment whole-body control scenarios. Specifically, we structure our experiments and ablation studies to address the following three principal research questions:

- **Q1:** Can the ANY2ANY successfully transfer diverse pretrained whole body tracking policies to novel robotic platforms with varying morphologies?
- **Q2:** What are the specific contributions and roles of the individual algorithmic components within the ANY2ANY architecture?
- **Q3:** Compared to training policies from scratch, what are the comparative advantages of ANY2ANY concerning its sensitivity to training data volume (sample efficiency) and overall computational efficiency?

### 4.1 Experimental Setup

#### 4.1.1 Cross-Embodiment Benchmark Design

We build our cross-embodiment benchmark on four humanoid platforms with different morphologies and kinematic configurations: LimX Oli [44], LimX Luna [45], Unitree G1 [46], and Unitree H1 [47]. LimX Oli is a 31-DoF full-size humanoid, while LimX Luna is also a full-size LimX humanoid but with a different 27-DoF configuration. Together with Unitree G1 and H1, these robots provide a diverse set of embodiments for evaluating cross-platform whole-body tracking adaptation.

We use two pretrained WBT policies as source backbones. The first is our self-pretrained **Oli-WBT**, trained on LimX Oli with over 500 hours of motion data using both Transformer and MLP backbones. The second is **Sonic**, an open-sourced WBT policy pretrained on Unitree G1. We evaluate two transfer directions: adapting Sonic to LimX Oli and LimX Luna, and adapting Oli-WBT to Unitree G1, Unitree H1, and LimX Luna. These adaptations are performed with limited target-side compute, using 4 NVIDIA A100 GPUs, to study how effectively pretrained WBT priors can be reused across different humanoid embodiments.

All adaptation experiments are driven by the AMASS [48] motion dataset, where human motions are retargeted to each target robot through General motion retargeting [21]. This unified setup enables consistent evaluation across different source policies and target embodiments while isolating the effectiveness of the proposed cross-embodiment adaptation framework.

#### 4.1.2 Baseline Design

To evaluate the effectiveness of the proposed cross-embodiment adaptation framework, we compare against several representative policy adaptation strategies built upon the same PPO training pipeline. Specifically, all methods share identical network architectures, training environments, reward functions, and motion retargeting pipelines.

As a primary baseline, we consider Training from Scratch. In this setting, the target embodiment policy is initialized randomly and trained directly using PPO on the retargeted AMASS dataset, without leveraging any pretrained model prior, which is specialized to a single target robot and does not incorporate any transferable knowledge from other embodiments. This baseline reflects the conventional humanoid reinforcement learning pipeline and serves as a reference for evaluating adaptation efficiency.

For parameter-efficient adaptation comparison experiments, we further incorporate **LoRA** [26], **Adapter** [27], and **Prefix-Tuning** [28], each adapting the pretrained WBT policy by introducing lightweight trainable modules while keeping most backbone parameters frozen.

### 4.1.3 Evaluation Metrics

We evaluate our method from two complementary perspectives. During training, we monitor the core WBT reward, namely the *tracking joint position* reward or *tracking body position* reward, and compare different methods in terms of both the converged reward value and the convergence efficiency, which together reflect the asymptotic tracking quality and the sample efficiency of the policy. During deployment in MuJoCo, we report the success rate of motion tracking, the Mean Per-Joint Position Error (MPJPE) that measures overall joint-level tracking fidelity, and the base position and orientation tracking errors in the world frame that characterize global motion accuracy. In addition, we report the mean magnitude of the velocity and acceleration of the policy output, which reflect the smoothness of the commanded actions and are indicative of the policy’s suitability for real-world deployment.

## 4.2 Cross-Embodiment Transfer Performance

To address **Q1**, we evaluate ANY2ANY on five concrete source-to-target transfer instances. The first group uses our Oli-pretrained WBT policy as the source backbone and adapts it to Unitree G1, Unitree H1, and LimX Luna, corresponding to OLIWBT2G1, OLIWBT2H1, and OLIWBT2LUNA. The second group uses Sonic, an open-source WBT policy pretrained on Unitree G1, and adapts it to LimX Oli and LimX Luna, corresponding to SONIC2OLI and SONIC2LUNA. In all cases, ANY2ANY is compared against a Specialist baseline trained from scratch on the target embodiment.

### 4.2.1 Sonic as Source Model

We further evaluate ANY2ANY with Sonic as an external pretrained WBT source policy. This gives two transfer instances, SONIC2OLI and SONIC2LUNA with only AMASS dataset. For Sonic adaptation, LoRA modules are inserted into the actor dynamics decoder and the critic network, while the FSQ module and other pretrained components remain frozen.

As shown in Figure 3, ANY2ANY adapts the Sonic policy substantially more efficiently than training the policy from scratch. Without retuning any reward coefficient, the total reward improves rapidly in the early stage and converges to a higher final value, and the gains are consistent across both anchor-position tracking and relative-body-position tracking, indicating that the transferred Sonic prior helps preserve global body motion as well as local whole-body configuration. The rollout snapshots further show stable tracking of diverse motions on Oli and Luna after adaptation.

### 4.2.2 Oli-WBT as Source Model

We first evaluate three ANY2ANY instances using the Oli-pretrained WBT policy as the source backbone: OLIWBT2G1, OLIWBT2H1, and OLIWBT2LUNA. All experiments use AMASS motions retargeted to each target robot by GMR and are trained on four A100 GPUs. As shown in Figure 4, ANY2ANY consistently outperforms the Specialist baseline across the three target embodiments. The radar plots show lower tracking errors on most joint- and body-level metrics, suggesting that the Oli-pretrained policy contains reusable whole-body motion priors. The reward curves fur-

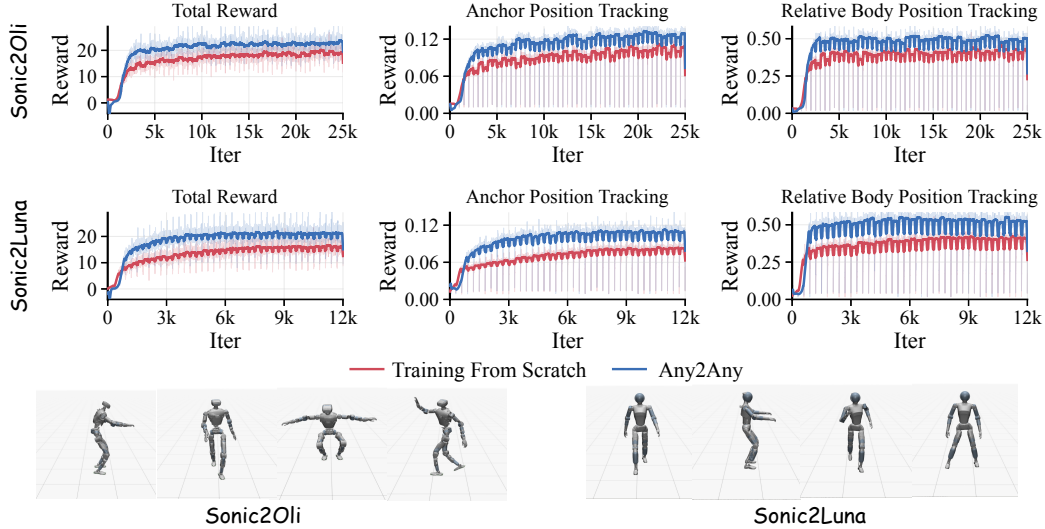


Figure 3: ANY2ANY transfer from Sonic to LimX humanoids, including SONIC2OLI and SONIC2LUNA. The curves compare ANY2ANY with the baseline, and the snapshots show stable rollout motions after adaptation.

ther demonstrate faster convergence: ANY2ANY rapidly reaches high tracking rewards in the early training stage and obtains higher or comparable final rewards.

The sim-to-sim snapshots verify that the adapted policies can stably execute diverse motions, including walking, running, manipulation, squatting, and bending down. These results indicate that ANY2ANY can efficiently adapt a pretrained WBT policy to humanoids with different morphologies without retraining whole-body control from scratch.

Together, these results demonstrate that ANY2ANY is not restricted to a specific pretrained backbone and can serve as a practical tool for transfer pretrained humanoid WBT policies across different humanoids.

### 4.3 Ablation Analyses

This section addresses **Q2** and **Q3**, which concern the internal design and practical efficiency of ANY2ANY. Sec. 4.3.1 addresses **Q2** by dissecting the role of each algorithmic component, including the necessity of kinematic calibration, the choice of parameter-efficient fine-tuning method, and the placement of LoRA modules within the frozen backbone. Sec. 4.3.2 addresses **Q3** by evaluating ANY2ANY under varying data scales and sampling budgets, which jointly characterize its data efficiency and compute efficiency relative to training from scratch. Unless otherwise specified, all ablations are conducted on OLIWBT2LUNA, a representative ANY2ANY instance with non-trivial morphological and kinematic discrepancies.

#### 4.3.1 Ablation on Architectural Components

To answer **Q2**, We conduct architectural ablations on the representative OLIWBT2LUNA transfer instance to analyze the two core components of ANY2ANY: kinematic alignment and parameter-efficient adaptation, using both Transformer and MLP backbones.

Figure 5(a) studies the effect of kinematic alignment. We compare four settings: training from scratch, full fine-tuning without alignment, full fine-tuning with alignment, and ANY2ANY with LoRA. Across both Transformer and MLP backbones, training from scratch converges slowly and reaches a lower final reward, indicating that learning whole-body tracking directly on the target embodiment remains data- and compute-intensive. Full fine-tuning without alignment improves over

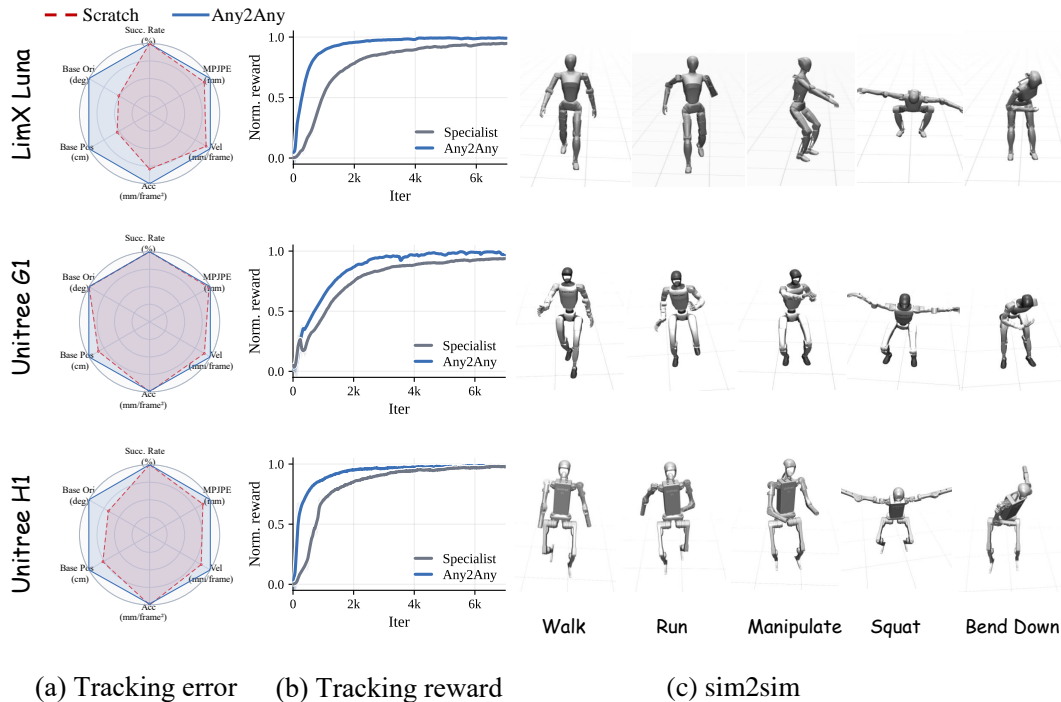


Figure 4: ANY2ANY transfer from the Oli-pretrained WBT policy to three target humanoids: OLIMX Luna, Unitree G1, and Unitree H1. ANY2ANY is compared with the baseline trained from scratch. (a) Tracking-error radar plots. (b) Training curves of normalized tracking reward. (c) Sim-to-sim rollouts on diverse motions.

scratch, but its convergence and final reward are still limited. This suggests that the pretrained WBT prior cannot be effectively reused when the target robot’s observations and actions are interpreted under inconsistent joint semantics. After kinematic alignment is introduced, full fine-tuning converges faster and achieves higher tracking rewards, confirming that aligning the observation, reference, and action spaces is necessary before transferring a pretrained policy across embodiments.

Notably, ANY2ANY with LoRA achieves performance comparable to aligned full fine-tuning while updating only a small fraction of the policy parameters. As shown in the table above Figure 5, LoRA reduces the trainable parameters from 100% to 5.26%, improves FPS from 34.8k to 111.7k, and lowers the collection cost from 21.10 to 7.51, while maintaining nearly the same joint and total rewards as full fine-tuning. These results show that, once kinematic semantics are aligned, adapting the entire pretrained policy is unnecessary: a lightweight low-rank update is sufficient to specialize the source WBT prior to the target embodiment.

Figure 5(b) further compares different PEFT mechanisms under the same aligned setting. LoRA consistently provides the best balance between training stability, convergence speed, and final performance for both Transformer and MLP backbones. Adapter tuning also improves over training from scratch, but converges more slowly and reaches lower rewards, suggesting that its additional bottleneck modules are harder to optimize in closed-loop whole-body control. Prefix tuning is the least stable: its reward either saturates at a low value or degrades during training, indicating that modifying only the input conditioning is insufficient to compensate for embodiment-level dynamical mismatch. Overall, these results support the design choice of ANY2ANY: kinematic alignment first establishes a shared semantic space, and LoRA then provides an efficient residual adaptation mechanism for the remaining embodiment-specific dynamics.

Method	Trainable Params↓	FPS↑	Collection Cost↓	Learning Cost↓	Joint Reward↑	Total Reward↑
Full FT (w/ align)	100.00%	34.8k	21.10	8.82	<b>1.64</b>	<b>22.67</b>
ANY2ANY (LoRA)	<b>5.26%</b>	<b>111.7k</b>	<b>7.51</b>	<b>7.60</b>	1.63	22.58

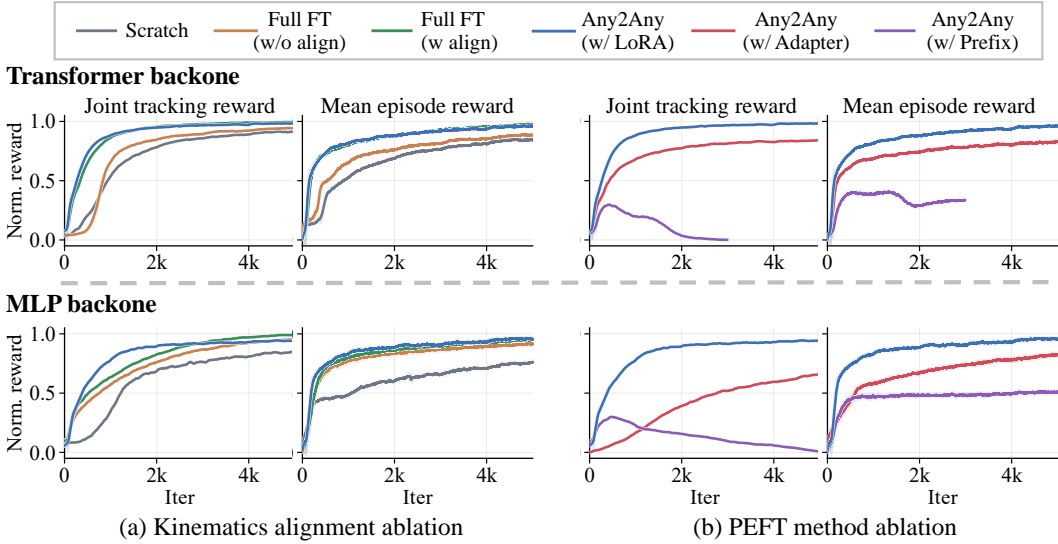


Figure 5: Ablation of ANY2ANY architectural components on OLIWBT2LUNA. The top table compares aligned full fine-tuning and ANY2ANY with LoRA. (a) Kinematic alignment ablation. (b) PEFT method ablation under kinematic alignment. ANY2ANY-LoRA achieves comparable rewards to full fine-tuning while using fewer trainable parameters and lower training cost.

Figure 6 further studies where the LoRA residual should be injected after kinematic alignment. The table groups the candidate injection sites into actor and critic components, including the actor backbone, reference input projection, proprioception input projection, action output projection, critic backbone, and critic input/output projections. This component-level ablation allows us to examine which parts of the pretrained WBT policy carry embodiment-agnostic motion priors and which parts require target-specific dynamic correction.

The results show that the injection location has a significant effect on both convergence and final tracking performance. Applying LoRA only to the actor backbone provides a useful baseline adaptation, confirming that the frozen pretrained policy contains reusable whole-body motion priors. However, adapting the backbone alone is not sufficient to fully compensate for the target embodiment. The best performance is achieved by S7, which applies

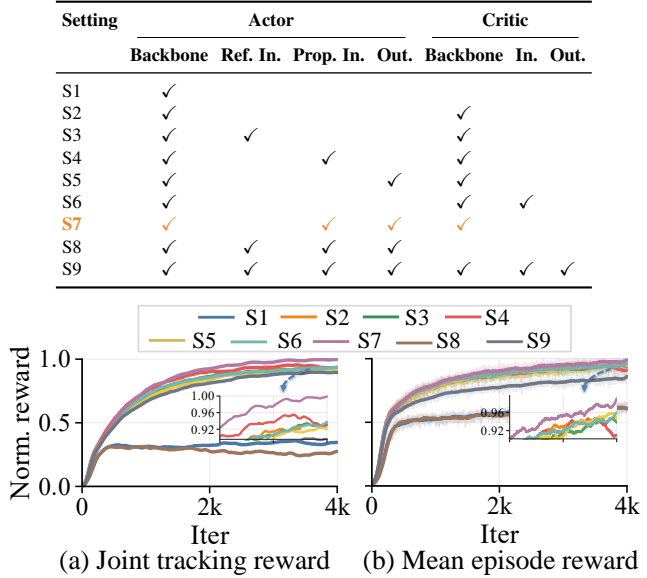


Figure 6: Ablation of LoRA injection scopes on OLIWBT2LUNA. The table summarizes the component-level injection locations across actor and critic modules, while the curves show the resulting joint tracking reward and mean episode reward.

Frames	Method	Base Pos. (cm)↓	MPIPE (mm)↓	Vel. (mm/f)↓
15M	Specialist	42.1	55.3	6.17
	Any2Any	<b>30.5</b>	<b>48.6</b>	<b>5.56</b>
7.5M	Specialist	60.3	59.9	6.28
	Any2Any	<b>44.1</b>	<b>57.9</b>	<b>5.86</b>
1.5M	Specialist	71.5	57.7	6.19
	Any2Any	<b>38.2</b>	<b>51.9</b>	<b>5.76</b>
0.4M	Specialist	79.5	61.8	6.31
	Any2Any	<b>51.9</b>	<b>56.9</b>	<b>6.02</b>
0.04M	Specialist	100.5	67.1	7.12
	Any2Any	<b>58.4</b>	<b>59.2</b>	<b>6.64</b>

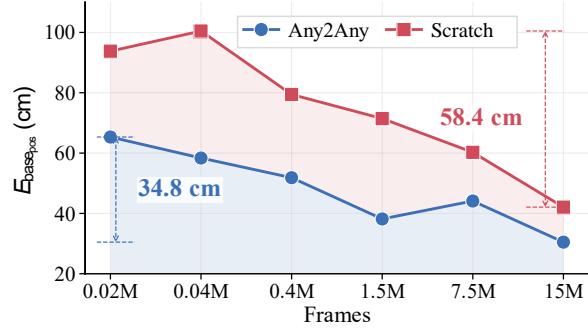


Figure 7: Performance comparison under varying data scales. Left: quantitative tracking errors. Right: base-position error across data scales.

LoRA to the actor backbone, actor proprioception input projection, actor output projection, and critic backbone. This indicates that the dominant residual mismatch after kinematic alignment lies in the dynamics-aware control pathway: the policy needs to reinterpret the target robot’s proprioceptive state and recent action history, and also adjust how the shared motion representation is decoded into target-specific joint commands.

This finding is consistent with the design principle of ANY2ANY. After the observation, reference, and action spaces are kinematically aligned, the reference-motion stream becomes relatively embodiment-agnostic and should be largely preserved. In contrast, the proprioception stream, action output head, and critic backbone are more directly coupled to the target robot’s mass distribution, actuator response, contact behavior, and closed-loop stability. Adapting these modules allows the policy to absorb the remaining dynamics residual while keeping the high-level WBT prior intact. Therefore, S7 provides the best trade-off between target-specific dynamic adaptation and preservation of reusable whole-body motion priors.

### 4.3.2 Ablation on Data and Compute Budget

To answer Q3, we evaluate ANY2ANY under different data scales and sampling rates. Figure 7 evaluates the data efficiency of ANY2ANY under controlled sampling conditions. We keep the sampling rate and training pipeline fixed, and vary only the scale of the 50Hz motion dataset, ranging from 0.02M to 15M frames. The table reports quantitative tracking errors, and the bottom curve visualizes the base-position error across data scales. As shown in Figure 7, ANY2ANY consistently achieves lower errors than the Specialist baseline across all data scales. The advantage becomes more pronounced in low-data regimes. For example, with only 0.04M frames, the Specialist reaches 100.5 cm base-position error, while ANY2ANY reduces it to 58.4 cm. These results indicate that the pretrained WBT prior provides reusable balance and coordination knowledge, allowing the target policy to learn embodiment-specific corrections from much less data instead of relearning whole-body control from scratch.

Figure 8 evaluates compute efficiency under different sampling rates, which correspond to different GPU settings: 16K with one RTX 4090, 32K with two RTX 4090s, 64K with four RTX 4090s, and 80K with four A100s. The two plots report the normalized joint tracking reward and mean episode reward. Figure 8 shows a similar trend under different sampling budgets. When reducing the sampling rate from 80K to 16K, Specialist drops by 18.6% in joint tracking reward and 16.4% in mean episode reward, while ANY2ANY drops by only 10.5%

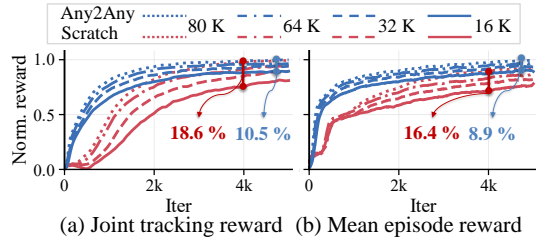


Figure 8: Comparison of reward curves under different GPU settings.

and 8.9%, indicating that training from scratch strongly depends on large-scale parallel sampling. In contrast, ANY2ANY is less sensitive to the reduced sampling budget. This suggests that the pre-trained WBT prior narrows the optimization search space, so the target robot only needs to learn embodiment-specific corrections rather than discovering whole-body control from scratch.

## 5 Conclusion

In this work, we present ANY2ANY, a novel paradigm for efficiently transferring pretrained WBT policies across humanoid embodiments. Addressing the challenges of large-scale WBT training, including high data requirements, significant computational cost, and embodiment-specific specialization, ANY2ANY first performs kinematic alignment to establish a consistent joint-level and observation-space correspondence between source and target robots. It then leverages dynamics adaptation to adapt the pretrained policy, preserving the motion priors of the source specialist while introducing lightweight, embodiment-specific updates for the target robot. We validate ANY2ANY on five concrete transfer instances. These experiments cover two different pretrained WBT source backbones and four humanoid platforms. These results demonstrate that the priors learned by pre-trained WBT specialists are not confined to a single robot embodiment, but can be efficiently and reliably transferred to diverse humanoid platforms. Overall, ANY2ANY provides a scalable and practical solution for deploying high-fidelity whole-body control on new humanoid robots, bridging the gap between pretrained models and real-world cross-embodiment applications.

## Acknowledgments

## References

- [1] Z. Luo, Y. Yuan, T. Wang, C. Li, S. Chen, F. Castaneda, Z.-A. Cao, J. Li, D. Minor, Q. Ben, et al. Sonic: Supersizing motion tracking for natural humanoid whole-body control. *arXiv preprint arXiv:2511.07820*, 2025.
- [2] M. Pirotta, A. Tirinzoni, A. Touati, A. Lazaric, and Y. Ollivier. Fast imitation via behavior foundation models. In *International Conference on Learning Representations*, volume 2024, pages 12685–12724, 2024.
- [3] M. Yuan, T. Yu, W. Ge, X. Yao, D. Li, H. Wang, J. Chen, B. Li, W. Zhang, W. Zeng, et al. A survey of behavior foundation model: Next-generation whole-body control system of humanoid robots. *IEEE transactions on pattern analysis and machine intelligence*, 2025.
- [4] E. Cetin, A. Touati, and Y. Ollivier. Finer behavioral foundation models via auto-regressive features and advantage weighting. *arXiv preprint arXiv:2412.04368*, 2024.
- [5] Y. Li, Z. Luo, T. Zhang, C. Dai, A. Kanervisto, A. Tirinzoni, H. Weng, K. Kitani, M. Guzek, A. Touati, et al. Bfm-zero: A promptable behavioral foundation model for humanoid control using unsupervised reinforcement learning. *arXiv preprint arXiv:2511.04131*, 2025.
- [6] Z. Gu, J. Li, W. Shen, W. Yu, Z. Xie, S. McCrory, X. Cheng, A. Shamsah, R. Griffin, C. K. Liu, et al. Humanoid locomotion and manipulation: Current progress and challenges in control, planning, and learning. *IEEE/ASME Transactions on Mechatronics*, 31(2):2300–2330, 2026.
- [7] X. Cheng, Y. Ji, J. Chen, R. Yang, G. Yang, and X. Wang. Expressive whole-body control for humanoid robots. *arXiv preprint arXiv:2402.16796*, 2024.
- [8] T. He, Z. Luo, X. He, W. Xiao, C. Zhang, W. Zhang, K. Kitani, C. Liu, and G. Shi. Omnih2o: Universal and dexterous human-to-humanoid whole-body teleoperation and learning. *arXiv preprint arXiv:2406.08858*, 2024.
- [9] Y. Ze, Z. Chen, J. P. Araújo, Z.-a. Cao, X. B. Peng, J. Wu, and C. K. Liu. Twist: Teleoperated whole-body imitation system. *arXiv preprint arXiv:2505.02833*, 2025.
- [10] Z. Chen, M. Ji, X. Cheng, X. Peng, X. B. Peng, and X. Wang. Gmt: General motion tracking for humanoid whole-body control. *arXiv preprint arXiv:2506.14770*, 2025.
- [11] A. Gupta, L. Fan, S. Ganguli, and L. Fei-Fei. Metamorph: Learning universal controllers with transformers. *arXiv preprint arXiv:2203.11931*, 2022.
- [12] S. Yang, Z. Fu, Z. Cao, G. Junde, P. Wensing, W. Zhang, and H. Chen. Multi-loco: Unifying multi-embodiment legged locomotion via reinforcement learning augmented diffusion. *arXiv preprint arXiv:2506.11470*, 2025.
- [13] Y. Xue, Y. Lin, W. Dong, Y. Tang, J. Wang, J. Pang, M. Zhou, M. Liu, and W. Zhang. Scalable and general whole-body control for cross-humanoid locomotion. *arXiv preprint arXiv:2602.05791*, 2026.
- [14] M. Liu, D. Pathak, and A. Agarwal. Locoformer: Generalist locomotion via long-context adaptation. In *Proceedings of The 9th Conference on Robot Learning*, 2025.
- [15] S. Yang, Z. Fu, Z. Cao, J. Guo, P. Wensing, W. Zhang, and H. Chen. Multi-loco: Unifying multi-embodiment legged locomotion via reinforcement learning augmented diffusion. *arXiv preprint arXiv:2506.11470*, 2025.
- [16] J. Bjorck, F. Castañeda, N. Cherniadev, X. Da, R. Ding, L. Fan, Y. Fang, D. Fox, F. Hu, S. Huang, et al. Gr00t n1: An open foundation model for generalist humanoid robots. *arXiv preprint arXiv:2503.14734*, 2025.

- [17] H. Luo, Y. Wang, W. Zhang, S. Zheng, Z. Xi, C. Xu, H. Xu, H. Yuan, C. Zhang, Y. Wang, et al. Being-h0.5: Scaling human-centric robot learning for cross-embodiment generalization. *arXiv preprint arXiv:2601.12993*, 2026.
- [18] S. Bai, M. Li, X. Lv, J. Wang, X. Wang, F. Liao, C. Hou, L. Gu, W. Zhou, K. Wu, et al. Hex: Humanoid-aligned experts for cross-embodiment whole-body manipulation. *arXiv preprint arXiv:2604.07993*, 2026.
- [19] D. Kim, J. Lee, J. Ahn, O. Campbell, H. Hwang, and L. Sentis. Computationally-robust and efficient prioritized whole-body controller with contact constraints. In *2018 IEEE/RSJ International Conference on Intelligent Robots and Systems (IROS)*, pages 1–8. IEEE, 2018. doi:10.1109/IROS.2018.8593767.
- [20] M. Chignoli, D. Kim, E. Stanger-Jones, and S. Kim. The mit humanoid robot: Design, motion planning, and control for acrobatic behaviors. In *2020 IEEE-RAS 20th International Conference on Humanoid Robots (Humanoids)*, pages 1–8. IEEE, 2021. doi:10.1109/HUMANOIDS47582.2021.9555782.
- [21] J. P. Araujo, Y. Ze, P. Xu, J. Wu, and C. K. Liu. Retargeting matters: General motion retargeting for humanoid motion tracking. *arXiv preprint arXiv:2510.02252*, 2025.
- [22] W. Zeng, S. Lu, K. Yin, X. Niu, M. Dai, J. Wang, and J. Pang. Behavior foundation model for humanoid robots. *arXiv preprint arXiv:2509.13780*, 2025.
- [23] T. Zhu, G. Cai, Y. Zhaohui, G. Ren, H. Xie, Z. Wang, J. Wu, J. Wang, X. Yang, Y. Mu, et al. Clot: Closed-loop global motion tracking for whole-body humanoid teleoperation. *arXiv preprint arXiv:2602.15060*, 2026.
- [24] M. Chen, K. Wang, B. Zhang, X. Ma, Z. Yang, Y. Ren, Q. Huang, Z. Zhu, Y. Wang, and Z. Su. Holomotion-1 technical report. *arXiv preprint arXiv:2605.15336*, 2026.
- [25] N. Ding, Y. Qin, G. Yang, F. Wei, Z. Yang, Y. Su, S. Hu, Y. Chen, C.-M. Chan, W. Chen, et al. Parameter-efficient fine-tuning of large-scale pre-trained language models. *Nature Machine Intelligence*, 5(3):220–235, 2023. doi:10.1038/s42256-023-00626-4. URL <https://www.nature.com/articles/s42256-023-00626-4>.
- [26] E. J. Hu, Y. Shen, P. Wallis, Z. Allen-Zhu, Y. Li, S. Wang, L. Wang, and W. Chen. Lora: Low-rank adaptation of large language models. In *International Conference on Learning Representations*, 2022. URL <https://openreview.net/forum?id=nZeVKeeFYf9>.
- [27] N. Houlsby, A. Giurgiu, S. Jastrzebski, B. Morrone, Q. de Laroussilhe, A. Gesmundo, M. Attariyan, and S. Gelly. Parameter-efficient transfer learning for nlp. In *International Conference on Machine Learning*, pages 2790–2799, 2019. URL <https://arxiv.org/abs/1902.00751>.
- [28] X. L. Li and P. Liang. Prefix-tuning: Optimizing continuous prompts for generation. In *Proceedings of the 59th Annual Meeting of the Association for Computational Linguistics*, pages 4582–4597, 2021. doi:10.18653/v1/2021.acl-long.353. URL <https://aclanthology.org/2021.acl-long.353/>.
- [29] X. B. Peng, P. Abbeel, S. Levine, and M. van de Panne. Deepmimic: Example-guided deep reinforcement learning of physics-based character skills. *ACM Transactions on Graphics*, 37(4):1–14, 2018. doi:10.1145/3197517.3201311. URL <https://arxiv.org/abs/1804.02717>.
- [30] Z. Luo, J. Cao, A. Winkler, K. Kitani, and W. Xu. Perpetual humanoid control for real-time simulated avatars. In *Proceedings of the IEEE/CVF International Conference on Computer Vision (ICCV)*, 2023. URL [https://openaccess.thecvf.com/content/ICCV2023/html/Luo\\_Perpetual\\_Humanoid\\_Control\\_for\\_Real-time\\_Simulated\\_Avatars\\_ICCV\\_2023\\_paper.html](https://openaccess.thecvf.com/content/ICCV2023/html/Luo_Perpetual_Humanoid_Control_for_Real-time_Simulated_Avatars_ICCV_2023_paper.html).

- [31] Y. Li, Y. Lin, J. Cui, T. Liu, W. Liang, Y. Zhu, and S. Huang. Clone: Closed-loop whole-body humanoid teleoperation for long-horizon tasks. In *Proceedings of The 9th Conference on Robot Learning*, 2025. URL <https://arxiv.org/abs/2506.08931>.
- [32] Y. Pan, R. Qiao, L. Chen, K. Chitta, L. Pan, H. Mai, Q. Bu, H. Zhao, C. Zheng, P. Luo, et al. Agility meets stability: Versatile humanoid control with heterogeneous data. *arXiv preprint arXiv:2511.17373*, 2025.
- [33] Z. Sun, B.-S. Huang, Y. Peng, X. Li, J. Ma, Y. Sun, Z. Li, H. Jiang, B. Gao, Z. Bing, et al. Mosaic: Bridging the sim-to-real gap in generalist humanoid motion tracking and teleoperation with rapid residual adaptation. *arXiv preprint arXiv:2602.08594*, 2026.
- [34] Y. Wang, S. Zhu, P. Zhi, Y. Li, J. Li, Y.-L. Li, Y. Xiao, X. Wang, B. Jia, and S. Huang. Omnixtreme: Breaking the generality barrier in high-dynamic humanoid control. *arXiv preprint arXiv:2602.23843*, 2026.
- [35] Y. Lin, M. Liu, Y. Xue, M. Zhou, Y. Yu, J. Pang, and W. Zhang. H-zero: Cross-humanoid locomotion pretraining enables few-shot novel embodiment transfer. *arXiv preprint arXiv:2512.00971*, 2025. URL <https://arxiv.org/abs/2512.00971>.
- [36] Open X-Embodiment Collaboration, A. O’Neill, A. Rehman, A. Gupta, A. Maddukuri, A. Gupta, A. Padalkar, A. Lee, A. Pooley, A. Gupta, et al. Open x-embodiment: Robotic learning datasets and rt-x models. In *Proceedings of the IEEE International Conference on Robotics and Automation (ICRA)*, pages 6892–6903, 2024. doi:10.1109/ICRA57147.2024.10611477. URL <https://arxiv.org/abs/2310.08864>.
- [37] Octo Model Team, D. Ghosh, H. Walke, K. Pertsch, K. Black, O. Mees, S. Dasari, J. Hejna, T. Kreiman, C. Xu, J. Luo, Y. L. Tan, L. Y. Chen, P. Sanketi, Q. Vuong, T. Xiao, D. Sadigh, C. Finn, and S. Levine. Octo: An open-source generalist robot policy. In *Proceedings of Robotics: Science and Systems (RSS)*, 2024. doi:10.15607/RSS.2024.XX.090. URL <https://arxiv.org/abs/2405.12213>.
- [38] J. Bjorck, F. Castaneda, N. Cherniadev, X. Da, R. Ding, L. Fan, Y. Fang, D. Fox, F. Hu, S. Huang, et al. GR00T N1: An open foundation model for generalist humanoid robots. *arXiv preprint arXiv:2503.14734*, 2025. URL <https://arxiv.org/abs/2503.14734>.
- [39] H. Luo, Y. Wang, W. Zhang, S. Zheng, Z. Xi, C. Xu, H. Xu, H. Yuan, C. Zhang, Y. Wang, Y. Feng, and Z. Lu. Being-H0.5: Scaling human-centric robot learning for cross-embodiment generalization. *arXiv preprint arXiv:2601.12993*, 2026. URL <https://arxiv.org/abs/2601.12993>.
- [40] J. Devlin, M.-W. Chang, K. Lee, and K. Toutanova. BERT: Pre-training of deep bidirectional transformers for language understanding. In *Proceedings of the 2019 Conference of the North American Chapter of the Association for Computational Linguistics: Human Language Technologies*, pages 4171–4186. Association for Computational Linguistics, 2019. doi:10.18653/v1/N19-1423. URL <https://aclanthology.org/N19-1423/>.
- [41] N. Houlsby, A. Giurghi, S. Jastrzebski, B. Morrone, Q. de Laroussilhe, A. Gesmundo, M. Attariyan, and S. Gelly. Parameter-efficient transfer learning for nlp. In *Proceedings of the 36th International Conference on Machine Learning*, volume 97 of *Proceedings of Machine Learning Research*, pages 2790–2799. PMLR, 2019. URL <https://proceedings.mlr.press/v97/houlsby19a.html>.
- [42] M. J. Kim, C. Finn, and P. Liang. Fine-tuning vision-language-action models: Optimizing speed and success, 2025.
- [43] Y. Wang, P. Ding, L. Li, C. Cui, Z. Ge, X. Tong, W. Song, H. Zhao, W. Zhao, P. Hou, S. Huang, Y. Tang, W. Wang, R. Zhang, J. Liu, and D. Wang. V1a-adapter: An effective paradigm for tiny-scale vision-language-action model, 2025.

- [44] LimX Dynamics. LimX Oli: Full-Size General-Purpose Humanoid Robot. <https://www.limxdynamics.com/en/products/oli>, 2025. Accessed: 2026-05-22.
- [45] LimX Dynamics. LimX Luna Humanoid Robot. [https://x.com/LimX\\_Dynamics](https://x.com/LimX_Dynamics), 2026. Official product page not yet publicly available at the time of access; accessed: 2026-05-22.
- [46] Unitree Robotics. Unitree G1 Humanoid Robot. <https://www.unitree.com/g1>, 2024. Accessed: 2026-05-22.
- [47] Unitree Robotics. Unitree H1 Universal Humanoid Robot. <https://www.unitree.com/h1>, 2023. Accessed: 2026-05-22.
- [48] N. Mahmood, N. Ghorbani, N. F. Troje, G. Pons-Moll, and M. J. Black. Amass: Archive of motion capture as surface shapes. In *Proceedings of the IEEE/CVF international conference on computer vision*, pages 5442–5451, 2019.